

POSSIBLE LOCAL SPIRAL COUNTERPARTS TO COMPACT BLUE GALAXIES AT INTERMEDIATE REDSHIFT

ELIZABETH J. BARTON AND LIESE VAN ZEE

Herzberg Institute of Astrophysics, National Research Council of Canada, 5071 W. Saanich Rd., Victoria, BC, Canada V9E 2E7 (email: Betsy.Barton@hia.nrc.ca)

To appear in ApJ Letters

ABSTRACT

We identify nearby disk galaxies with optical structural parameters similar to those of intermediate-redshift compact blue galaxies. By comparing H I and optical emission-line widths, we show that the optical widths substantially underestimate the true kinematic widths of the local galaxies. By analogy, optical emission-line widths may underrepresent the masses of intermediate- z compact objects. For the nearby galaxies, the compact blue morphology is the result of tidally-triggered central star formation: we argue that interactions and minor mergers may cause apparently compact morphology at higher redshift.

Subject headings: galaxies: compact — galaxies: evolution — galaxies: interactions — galaxies: individual (CGCG 132-062, UGC 8919N) — galaxies: kinematics and dynamics — galaxies: structure

1. INTRODUCTION

Blue galaxies are abundant at intermediate redshift. Many are luminous, with distinct irregular or compact morphology (Phillips et al. 1997) and high rates of star formation. Number counts indicate they are the most strongly evolving population at intermediate redshift [Lilly et al. (1995); Ellis (1997) and references therein]. Thus, a complete understanding of galaxy evolution from $z = 1$ to the present requires understanding what stage of evolution the luminous blue galaxies represent.

The most extreme luminous blue galaxies at intermediate redshift are the compact narrow emission-line galaxies (CNELGs hereafter; Koo et al. 1994, 1995; Guzmán et al. 1996, 1997, 1998). With small half-light radii (1 – 3.5 kpc) and narrow emission-line velocity widths ($35 \lesssim \sigma < 126 \text{ km s}^{-1}$ from spatially unresolved spectra), CNELGs resemble few nearby objects. Their nature is currently heavily debated. Several authors (e.g., Koo et al. 1994, 1995) argue that the narrow emission-line widths of CNELGs indicate small masses; Koo et al. (1995) suggest CNELGs are the starbursting spheroidals faded by 4 – 7 magnitudes at the current epoch. However, spectroscopic studies of field galaxies at intermediate redshift (Carollo & Lilly 2000) and of compact objects in particular (Kobulnicky & Zaritsky 1999; Hammer et al. 2000) find high metallicities for some blue galaxies, suggesting that some, including some CNELGs, may be bulges forming with central bursts of star formation in luminous spirals.

At the heart of the debate is the question of the masses of the luminous compact blue galaxies. Additional kinematic information for the CNELGs, such as H I linewidths or stellar kinematics, would dramatically improve our knowledge of these systems. However, 21cm measurements are nearly impossible at intermediate z and any older stellar populations of CNELGs are too faint to measure stellar kinematics. One remaining avenue is study of local counterparts with properties similar to those of the CNELGs (e.g., Pisano et al. 2000).

Recently, Barton et al. (2001) identified a class of possible nearby counterparts to CNELGs and other lumi-

nous compact galaxies. The local galaxies are spirals in pairs with blue star-forming centers, small half-light radii, and anomalously narrow emission-line rotation widths. In these cases, concentrated line emission probably results from gas infall after a close galaxy-galaxy interaction, a process similar to central star formation triggered in minor mergers (Mihos & Hernquist 1994, 1996). Here, we argue that observations of these possible counterparts strongly support the hypothesis that at least some luminous blue compact galaxies at high redshift are disk galaxies with central star formation. In Sec. 2, we detail the evidence that these local objects are counterparts to compact blue galaxies at intermediate redshift. In Sec. 3, we present H I synthesis observations of two of the four galaxies which show that even resolved major axis emission-line rotation curves underrepresent the full kinematic widths of the local galaxies by more than a factor of two, allowing the possibility that in spite of their narrow emission-line widths, CNELGs are the centers of intrinsically massive systems. We conclude in Sec. 4. We use $H_0 = 50 \text{ km s}^{-1} \text{ Mpc}^{-1}$ and, where applicable, $q_0 = 0.1$.

2. LOCAL DISK GALAXIES WITH BLUE CENTERS

If luminous blue compact morphology is a brief transitional stage in massive galaxies, local counterparts may exist among galaxies that are rapidly evolving at the current epoch, such as galaxies in pairs. Many studies of the stellar populations of paired galaxies identify substantial new star formation triggered by interactions (e.g., Larson & Tinsley 1978; Kennicutt et al. 1987). Recently, Barton, Geller, & Kenyon (2000a) studied a large sample of galaxies in pairs selected from the CfA2 redshift survey based only on separation on the sky ($\leq 50 \text{ h}^{-1} \text{kpc}$) and in redshift ($\leq 1000 \text{ km s}^{-1}$). New spectra of 502 of the galaxies show that indicators of recent star formation, such as H α equivalent width, correlate with pair separation on the sky and in redshift, providing unambiguous evidence that close galaxy-galaxy passes trigger central star formation (Barton, Geller, & Kenyon 2000a). Subsequent B and R photometry of 190 galaxies in the sample indicates that

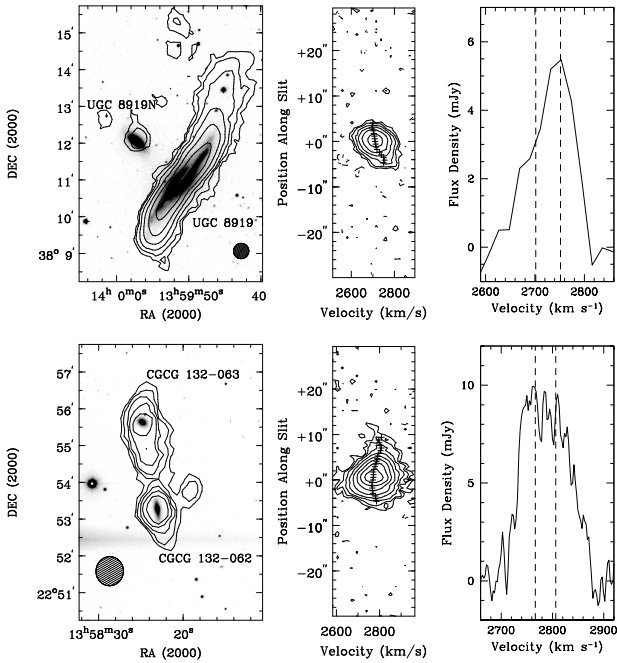


FIG. 1.— Images, rotation curves, and H I profiles of two candidates for counterparts to CNELGs selected from galaxies in pairs. The targets are UCG 8919N and CGCG 132-062. The left panels show B images (greyscale) and H I distributions (contours). The middle panels show the H α emission along the major axes of the targets, on an expanded spatial scale; the emission is centrally concentrated. Crosses mark the rotation curve derived from cross correlation analysis. The right panels show “single-dish” H I profiles for the local counterparts (solid lines); vertical dashed lines denote the optical rotation widths.

flux from the new stars can dominate even the *R*-band light in the centers of the galaxies (Barton, Geller, & Kenyon 2000b). This strong centralized star formation renders many of the paired galaxies good candidates for counterparts to the intermediate- z systems. Because the CNELGs and the other luminous compact objects have narrow emission lines, the emission-line kinematics provide the true test.

Barton et al. (2001) study the resolved emission-line rotation curves of 90 galaxies in the pair sample. Most lie on the Tully-Fisher (Tully & Fisher 1977, T-F hereafter) relation for non-interacting galaxies (e.g., Courteau 1997). However, they identify seven galaxies which, like the compact objects observed at higher redshifts, appear significantly “overluminous” for their measured emission-line widths.

2.1. Optical Observations of the Local Tully-Fisher Outliers

Four of the “overluminous” T-F outliers have properties similar to those of the compact blue objects selected from the Hubble deep field (Phillips et al. 1997). [The anomalous properties of the remaining three outliers probably result from tidal and gasdynamical distortion (Barton et al. 2001).] Table 1 lists the optical properties of the four local galaxies measured from *B* and *R* images and moderate-resolution major axis spectra; Barton et al. (2001) describe the data in more detail. Three of the four

are clearly disk galaxies; NGC 2719A is somewhat amorphous. Fig. 1 shows the images and rotation curves for UGC 8919N and CGCG 132-062, the two galaxies with H I synthesis observations. We measure total magnitudes and correct them for internal extinction as described in Barton et al. (2001). For direct comparison with the higher redshift objects, we use circular apertures to measure the *B*-band half-light radius, R_e .

Table 1 includes two different measures of the velocity widths of the galaxies from optical spectroscopy, $V_{2.2}$ and σ . $V_{2.2}$ is the spatially resolved emission-line rotation curve velocity width from Courteau (1997). It is the full width of the rotation curve at 2.15 disk scale lengths, from a model fit to the data; $V_{2.2}^c$ is corrected for observational effects, such as inclination, as in Barton et al. (2001). The small measured velocity widths reflect the fact that the strongest line emission is not spatially extended (see Fig 1).

The second velocity width measure, σ , is more directly comparable to existing measurements for higher-redshift objects. Because it is difficult to resolve the intermediate- z galaxies from the ground, the existing intermediate- z emission-line measurements of the compact objects include flux from the whole galaxy. In addition, the quoted linewidths are usually velocity dispersion measurements of Gaussian fits to the [OII], [OIII], or H β emission lines (Koo et al. 1995; Guzmán et al. 1996, 1997; Phillips et al. 1997). To approximate these measurements, we collapse the H α flux along the entire major axis and fit a Gaussian function to the H α line to measure σ . We measure the resolution of each observation from Gaussian fits to multiple sky lines in the extracted region. The resolutions range from 1.4–1.5 Å FWHM ($\sigma_{\text{RES}} = 26–29$ km s $^{-1}$ at H α). We apply the prescription of Guzmán et al. (1997) to account for instrumental resolution.

2.2. Comparison with Luminous Blue Compact Galaxies at Intermediate Redshift

The intrinsic masses of intermediate-redshift compact objects are uncertain. Bulk scaling parameters are frequently the only available measures. Fig. 2 shows an example of the use of these parameters; following Guzmán et al. (1996), we plot the half-light radii and velocity widths of compact objects (solid points: Koo et al. 1994, 1995; Guzmán et al. 1996, 1997, 1998; Phillips et al. 1997, and references therein). The open points are the local Frei et al. (1996) sample, which consists largely of massive galaxies; half-light radii are from Bershady, Jangren, & Conselice (2000) and σ comes from approximate values of σ based on H I measurements ($\sigma_{\text{RADIO}} = W_{50}/2.35$) compiled from the RC3 (de Vaucouleurs et al. 1991) and NED.¹ The four asterisks are the targets of this study, with σ measured from the optical emission-line widths (see σ in Table 1). This analysis, and similar plots of M_B vs. σ and M_B vs. R_e , place the local targets of the present study in the same range as many of the compact Hubble deep field objects (Phillips et al. 1997); they are less luminous than typical CNELGs.

The compact objects and CNELGs fall to the lower left of the majority of the Frei sample in Fig. 2. Although

¹The NASA/IPAC Extragalactic Database (NED) is operated by the Jet Propulsion Laboratory, California Institute of Technology, under contract with the National Aeronautics and Space Administration.

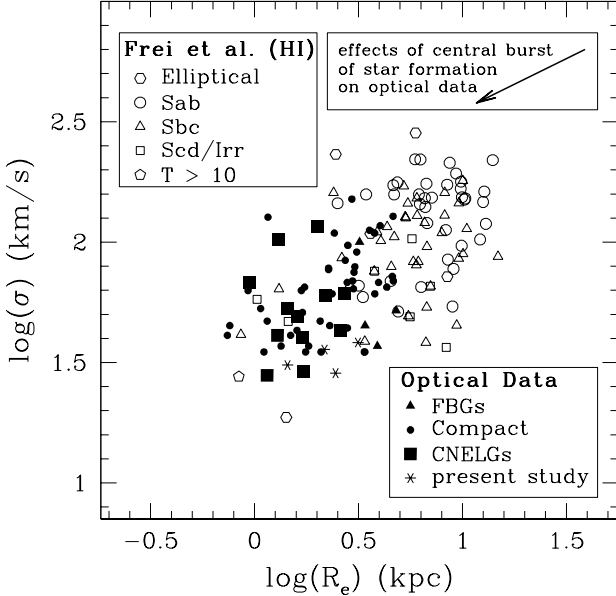


FIG. 2.— Structural parameters of intermediate- z compact objects (filled points), local galaxies (open points), and the proposed local counterparts to compact blue galaxies (asterisks). The overall trend is that smaller galaxies have smaller velocity dispersions. However, the arrow shows the effects of a central burst of star formation, which can “artificially” lower both the half-light radius and the optical emission-line width of the galaxy.

these scaling parameters seem to indicate that they are dwarf-like objects, this argument may be entirely flawed. The structural parameters (e.g., R_e) and the optical emission-line kinematics (both σ and $V_{2,2}$) are heavily influenced by regions of current and recent star formation; Fig. 3 shows a simple model for the effects of a bulge-forming central starburst. We model the disk with an exponentially decreasing star formation rate ($\tau = 4$ Gyr). At 7 Gyr (i.e., at intermediate redshift), a starburst forms an exponential bulge. We use the Bruzual & Charlot (1996, in preparation) star-formation models normalized for a bulge-to-disk ratio of 0.1 at the present day (14 Gyr here). The top panel shows the B -band half-light radius of the galaxy, adopting a bulge half-light radius $R_{e,b} = 0.5$ kpc, typical for exponential bulges (Carollo 1999), and a disk half-light radius of $12.5 R_{e,b}$, typical for late-type spirals (Courteau, de Jong, & Broeils 1996). The forming bulge dominates the flux and dramatically reduces the half-light radius. During bulge formation the system looks like the luminous compact, blue galaxies at intermediate redshift. With the additional assumptions of a fixed maximal-disk rotation curve, an inclination of 60° , and a linear dependence between star formation rate and $H\alpha$ flux, the bottom panel shows the decrease in the measured linewidth during the burst (see also Lehnert & Heckman 1996; Bershady & Mihos 2001). In summary, Fig. 3 shows that central star formation in the amount required to form a small bulge in a single burst can lower the measured half-light radius of a galaxy by a large amount (0.86 dex in Fig. 2) and can simultaneously lower the measured σ , by > 0.2 dex, shifting the object in Fig. 2 as shown by the arrow.

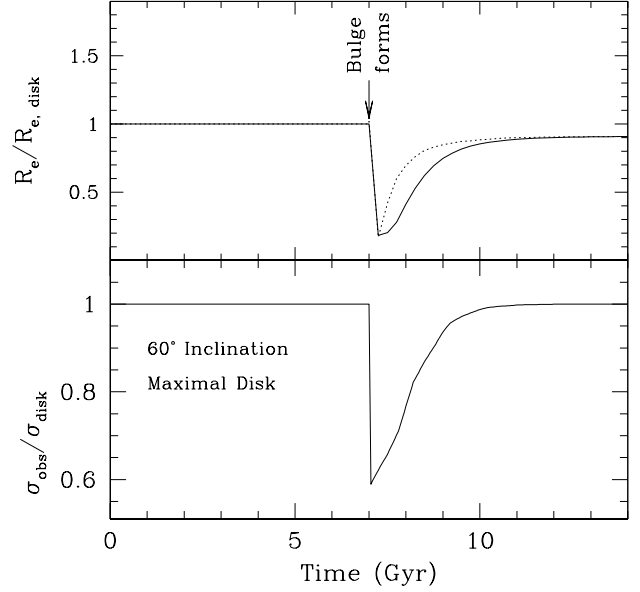


FIG. 3.— A simple model for how a bulge-forming central burst of star formation, either instantaneous (dotted line) or extended ($\tau = 500$ Myr, solid line), could temporarily decrease both the half-light radius (top) and σ (bottom) of a spiral galaxy. The model follows the disk from 14 Gyr ago through a bulge formation event at 7 Gyr to the present day. See the text for a description.

3. H I OBSERVATIONS: A BETTER PROBE OF THE KINEMATICS

Our local counterparts allow us to test the effects of central star formation on σ by comparing emission-line velocity widths in compact objects with H I observations (see also Kobulnicky & Gebhardt 2000; Pisano et al. 2000). Spatial separation of the galaxies in the pair required H I synthesis observations. We present Very Large Array² observations of two of the four objects in this study. We reduced archival observations of UGC 8919N originally obtained by J. Chengalur as part of a set of observations of UGC 8919, the larger galaxy in the pair. The archival data include both C and D-configuration observations obtained on 1993 July 23 and 1995 March 9. They totaled 257 minutes on-source in the C configuration and 118.5 minutes on-source in the D configuration, in 4IF mode with a bandwidth of 3.125 MHz. The two pairs of IFs were offset in frequency to provide full velocity coverage of UGC 8919. We observed CGCG 132-062 with the VLA in D configuration on 2000 August 18. The observations were conducted in 2AD mode with a frequency coverage of 1.56 MHz and on-line Hanning smoothing. We spent a total of 191 minutes on-source, with interspersed observations of phase and flux calibrators.

We followed standard data reduction practices, using tasks in the AIPS package to flux and phase calibrate the $u-v$ data (see, e.g., van Zee, Skillman, & Salzer 1998, for a full description of our standard reduction methods). CLEAN data cubes were created with the AIPS task IMAGR using robustness parameters from 5 (natural weight) to 0.5. Using the GIPSY software package, we constructed moment maps from clipped cubes consisting

²The Very Large Array is a facility of the National Radio Astronomy Observatory. The National Radio Astronomy Observatory is a facility of the National Science Foundation, operated under a cooperative agreement by Associated Universities Inc.

of regions with signal greater than 2 times the rms noise in at least 2 consecutive channels. The left-hand panels of Fig. 1 show the zeroth moment maps of the two systems; neither small galaxy is well resolved, but the line emission from each galaxy is easily identifiable and separable in the H I data cube. In addition to the known galaxy pair, one additional galaxy was identified in the data cube of CGCG 132-062 at a heliocentric velocity of 2860 km s^{-1} ; the coordinates correspond to the NED listing for MAP-NGP 0.381-0431360. We generated mock “single dish” H I profiles for each galaxy to derive the kinematic linewidths (Fig. 1). The H I linewidths listed in Table 1 were measured at the 50% of the peak points.

The 21cm lines of UGC 8919N and CGCG 132-062 are much wider than the collapsed major axis H α emission lines, with $\sigma/\sigma_{\text{RADIO}} = 0.67$ and 0.60, respectively. The W_{50} measurements are 102% and 202% wider, respectively, than the velocity widths ($V_{2.2}$) of the resolved rotation curves. The H I measurements shift the velocity widths upwards by ~ 0.2 dex in Fig. 2, similar to the amount predicted by the simple model of Fig. 3. The “true” (pre-burst) half-light radii may shift the galaxies into the spiral galaxy regime of Fig. 2.

4. TIDALLY-TRIGGERED GAS INFALL AND THE PHYSICS OF BLUE COMPACT MORPHOLOGY

Our study suggests that the central star formation triggered by gas infall after a close galaxy-galaxy pass is capable of causing discrepancies between H I and emission-line kinematics. Gas infall triggered by interactions (Mihos & Hernquist 1996) or minor mergers (Mihos & Hernquist 1994) is analogous to secular evolution (Pfenniger & Norman 1990). Thus, the process may explain the “exponential bulges” observed in some late-type spirals (e.g., Andredakis & Sanders 1994; Carollo 1999). If hierarchical scenarios of galaxy formation are correct, triggered gas infall may occur frequently at intermediate and high redshift. The bulge-forming spirals — especially the spirals with face-on inclinations or low surface brightness disks — would appear similar to compact objects already observed at higher redshifts.

For local galaxies, existing studies shed little light on

the frequency of these T-F outliers among non-interacting galaxies. Most T-F studies would exclude the targets of this study on the basis of morphology or because of poorly-sampled rotation curves. The existing studies do show that centrally concentrated star formation is not a sufficient condition for narrow emission lines. Several other galaxies in the Barton et al. (2001) study have centrally concentrated emission but are not outliers to the T-F relation. One explanation for the anomalous properties of these outliers is that the systems may have particularly shallow rotation curves. Thus, the observed rotation curve has a smaller total width when the new stars are centrally concentrated. In any case, these local galaxies demonstrate that centrally concentrated emission-line regions can, under some circumstances, lead to anomalously narrow emission lines in disk galaxies.

In summary, we identify a set of four nearby galaxies with blue centers, small half-light radii, and anomalously narrow emission-line widths that are possible counterparts to some of the compact blue galaxies observed at intermediate redshift. H I measurements, available for two of the galaxies, show that the emission-line widths underestimate the kinematic widths of the galaxies by $\gtrsim 50\%$. Thus, by analogy, the emission-line widths of the compact objects at intermediate redshift may underrepresent their masses. Because the local galaxies were selected from a sample of pairs, the physical mechanism responsible for their compact star formation is largely understood: a recent close galaxy-galaxy interaction drove gas from the disk into the center of each galaxy, triggering central star formation. This process, and the similar processes of minor mergers and secular evolution, may facilitate bulge formation. Thus, our study supports the hypothesis that at least some of the luminous compact blue galaxies with narrow emission lines observed at higher redshift are actually bulges forming in larger systems.

We thank John Salzer and Janice Lee for obtaining a preliminary H I spectrum of one of the targets for us in advance of the VLA observations. We thank Margaret Geller and David Crampton for useful comments and suggestions.

REFERENCES

Andredakis, Y. C., & Sanders, R. H. 1994, MNRAS, 267, 283
 Barton, E. J., Geller, M. J., & Kenyon, S. J. 2000a, ApJ, 530, 660
 Barton, E. J., Geller, M. J., & Kenyon, S. J. 2000b, in preparation
 Barton, E. J., Geller, M. J., Bromley, B. C., van Zee, L., & Kenyon, S. J. 2001, AJ, in press (astro-ph/0011022)
 Bershady, M. A., Jangren, A., & Conselice, C. J. 2000, AJ, 119, 2645
 Bershady, M. A., & Mihos, C. J. 2001, in preparation
 Carollo, M. C. 1999, ApJ, 523, 566
 Carollo, M. C., & Lilly, S. J. 2000, ApJ, in press (astro-ph/0011353)
 Courteau, S., de Jong, R. S., & Broeils, A. H. 1996, ApJ, 457, L73
 Courteau, S. C. 1997, AJ, 114, 2402
 de Vaucouleurs, G., de Vaucouleurs, A., Corwin, H. G., Buta, R., Paturel, G., & Fouqué, P. 1991, Third Reference Catalogue of Bright Galaxies (Springer, New York)
 Ellis, R. S. 1997, ARA&A, 35, 389
 Frei, Z., Guhathakurta, P., Gunn, J. E., & Tyson, J. A. 1996, AJ, 111, 174
 Guzmán, R., et al. 1996, ApJ, 460, L5
 Guzmán, R., et al. 1997, ApJ, 489, 559
 Guzmán, R., et al. 1998, ApJ, 495, L13
 Hammer, F., Gruel, N., Thuan, T. X., Flores, H., & Infante, L. 2000, ApJ, in press (astro-ph/0011218)
 Kennicutt, R. C., Jr., Keel, W. C., van der Hulst, J. M., Hummel, E., & Roettiger, K. A. 1987, AJ, 95, 5
 Kobulnicky, H. A., & Gebhardt, K. 2000, AJ, 119, 1608
 Kobulnicky, H. A., & Zaritsky, D. 1999, ApJ, 511, 118
 Koo, D. C., Bershady, M. A., Wirth, G. D., Stanford, S. A., & Majewski, S. R. 1994, ApJ, 427, L9
 Koo, D. C., et al. 1995, ApJ, 440, L49
 Larson, R. B., & Tinsley, B. M. 1978, ApJ, 219, 46
 Lehnert, M. D., & Heckman, T. M. 1996, ApJ, 472, 546
 Lilly, S. J., Tresse, L., Hammer, F., Crampton, D., & Le Fèvre, O. 1995, ApJ, 455, 108
 Mihos, J. C., & Hernquist, L. 1994, ApJ, 425, 12
 Mihos, J. C., & Hernquist, L. 1996, ApJ, 464, 641
 Pfenniger, D., & Norman, C. 1990, ApJ, 363, 391
 Phillips, A. C., et al. 1997, ApJ, 489, 543
 Pisano, D. J., Kobulnicky, H. A., Guzmán, R., & Gallego, J. 2000, in preparation
 Tully, R. B., & Fisher, J. R. 1977, A&A, 54, 661
 van Zee, L., Skillman, E. D., & Salzer, J. J. 1998, AJ, 116, 1186

TABLE 1
PROPERTIES OF THE LOCAL SAMPLE

Name	M_B	M_R	R_e (kpc)	$V_{2.2}$ (km s $^{-1}$)	$V_{2.2}^c$ (km s $^{-1}$)	σ (km s $^{-1}$)	W_{50} (km s $^{-1}$)	W_{50}^c (km s $^{-1}$)
UGC 8919N	-18.3	-19.4	3.52	50	64	29	101	112
CGCG 132-062	-18.0	-19.0	1.87	40	42	31	121	127
NGC 2719A	-18.5	-18.9	2.44	45	65	36	—	—
UGC 7085W	-19.3	-20.0	4.08	61	67	38	—	—